Electronic Supplementary information

An electron poor iridium pincer complex in catalytic alkane dehydrogenation

Oleksandr O. Kovalenko and Ola F. Wendt*

Centre for Analysis and Synthesis, Department of Chemistry, Lund University, P. O. Box 124,

S-221 00 Lund, Sweden. E-mail: ola.wendt@chem.lu.se

Contents

Table S1. Crystal data and refinement details for compounds **4, 5, 6** and **8**.

	4	**5**	**6**	**8**
Formula	$C_{24}H_{38}F_6O_2P_2$	$C_{24}H_{37}ClF_6IrO_2P_2$	$C_{16}H_{31}ClIrOP$	$C_{38}H_{57}F_6IrO_2P_2$
Fw	534.48	761.12	498.03	913.97
Space group	$P\,2_1/c$	$P\,2_1/c$	$P\,2_1/n$	$P\,2_1$
Crystal system	Monoclinic	Monoclinic	Monoclinic	Monoclinic
T/K	293(2)	293(2)	293(2)	293(2)
a□/Å	12.132(5)	8.318(5)	7.96730(10)	8.709(5)
b/Å	18.353(5)	31.333(5)	15.3786(2)	22.841(5)
c/Å	14.104(5)	12.075(5)	14.8875(3)	10.007(5)
β/deg	109.774(5)	109.444(5)	98.120(2)	92.394(5)
V/Å³	2955.2(18)	2968(2)	1805.82(5)	1988.9(16)
Z	4	4	4	2
D_{calcd} /g cm^{-3}	1.201	1.704	1.832	1.526
μ /mm^{-1}	0.202	4.754	7.625	3.496
θ-range /deg	2.935-28.838	2.904-28.719	2.902-28.869	2.943-28.803
No. reflns collected	33067	18421	19901	22511
No. of unique reflns	7037	6622	4335	9107
$R(F)$ $(I > 2$□$(I))$[a]	0.0649	0.0374	0.0334	0.0550
$wR^2(F^2)$ (all data)[b]	0.1841	0.0867	0.0666	0.1082
S[c]	1.018	1.033	1.054	1.018
R_{int}	0.0429	0.0279	0.0515	0.0783
CCDC	1478500	1478501	1478503	1478502
Flack param.				0.420(9)

[a] $R = \Sigma(|F_o| - |F_c|)/\Sigma|F_o|$. [b] $wR2 = [\Sigma w(F_o^2 - F_c^2)^2/\Sigma(F_o^2)^2]^{1/2}$.

[c] $S = [\Sigma w F_o^2 - F_c^2)^2/(n\text{-}p)]^{1/2}$.

Table S2. Catalytic activity of complex II in the transfer dehydrogenation of COA with TBE.

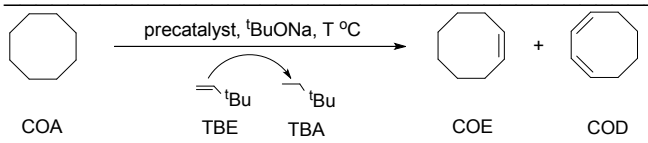

Entry[a]	t/h	TONs[b] II		Entry[a]	t/h	TONs[b] II
1	0,17	1136		7	8	1621
2	0,5	1346		8	15	1701
3	1	1435		9	24	1730
4	3	1499		10	40	1730
5	4	1530				
6	6	1581				

[a] Average of three runs, using a 3030:3030:1 ratio of COA/TBE/precatalyst and 1.5 equiv of tBuONa at 200 °C. All reactions were performed under an argon atmosphere.

[b] Determined by ^{1}H NMR, the sum of COE and COD double bonds equals TON of TBE within 2% difference.

Figure S1-1. ^{1}H NMR spectrum of **1,3-Dibromo-4,6-bis(trifluoromethyl)benzene (1)**

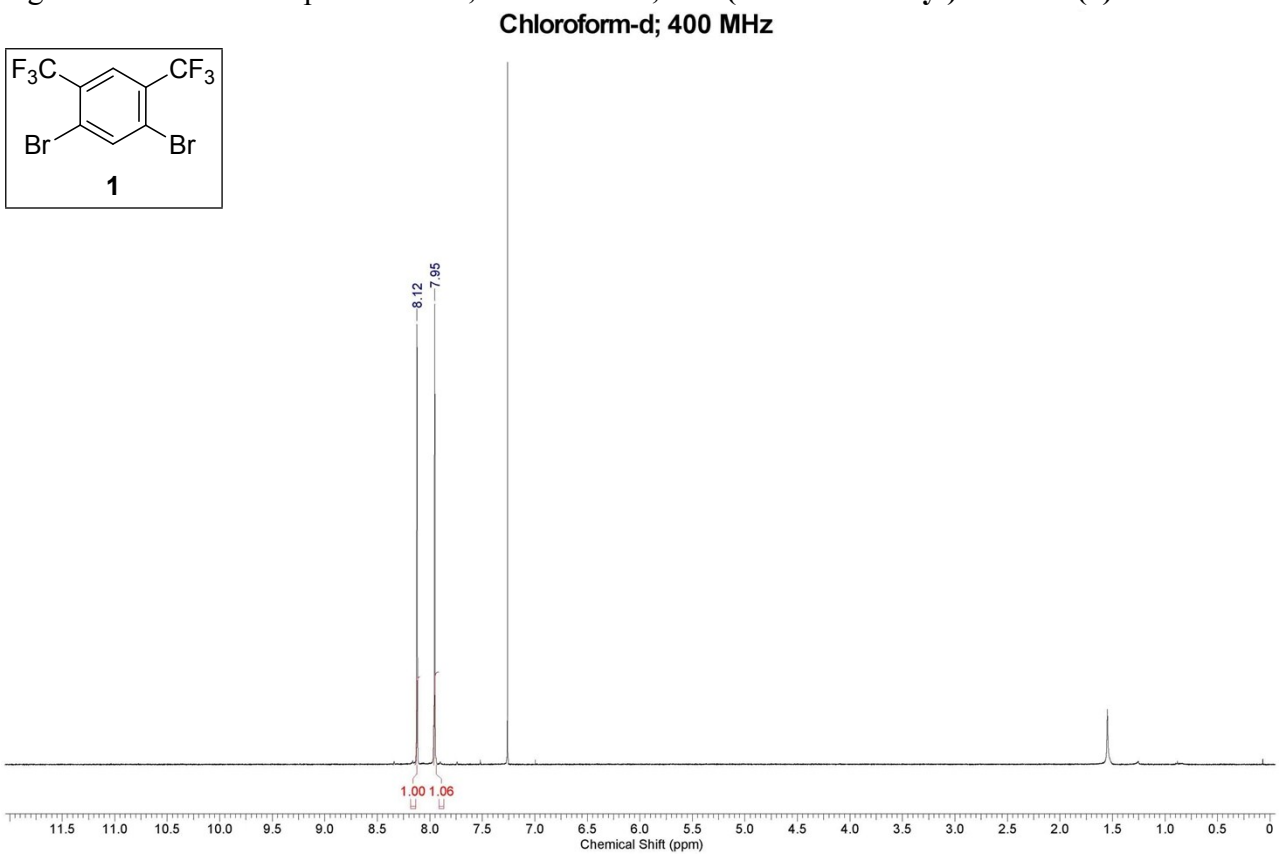

Figure S1-2. ^{19}F NMR spectrum of **1,3-Dibromo-4,6-bis(trifluoromethyl)benzene (1)**

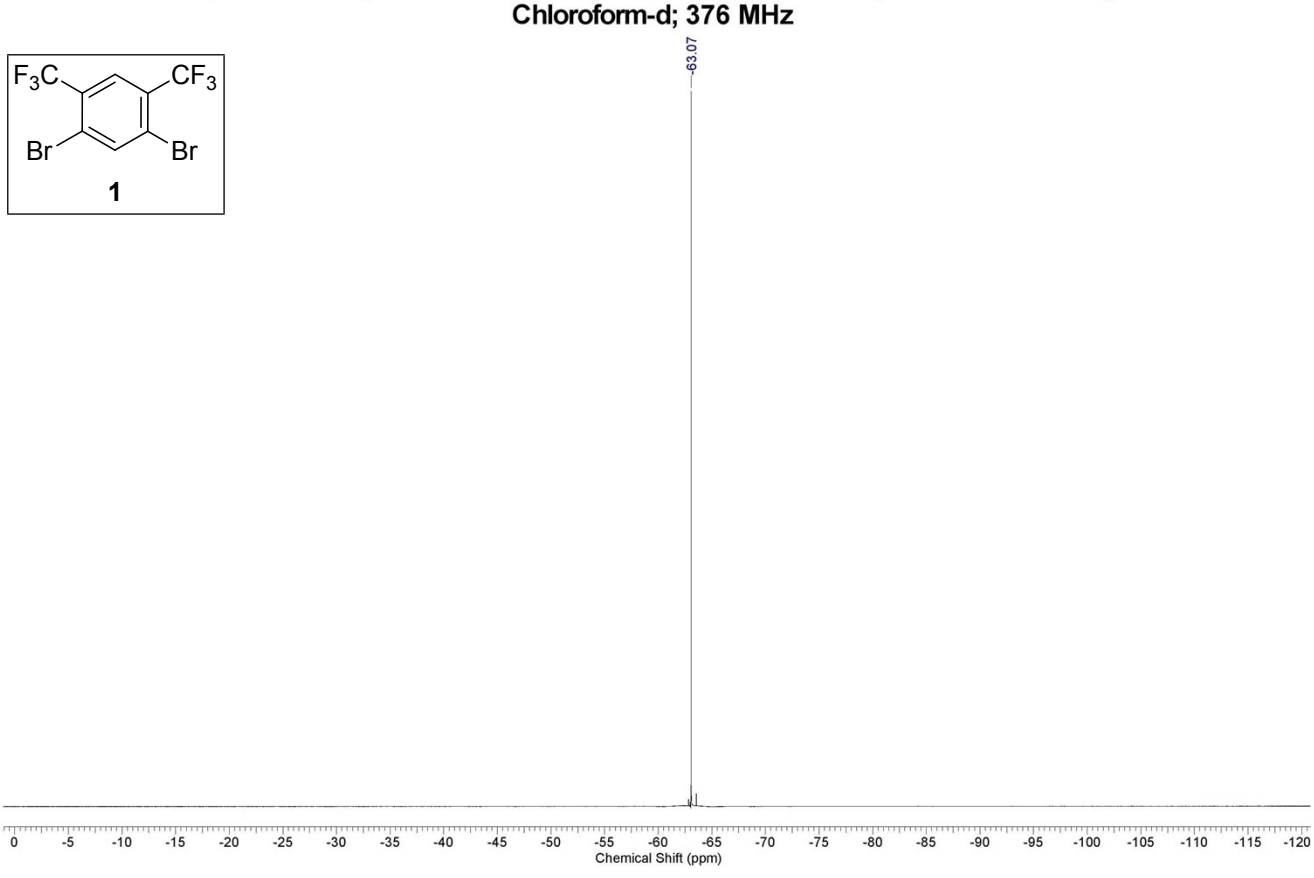

Figure S1-3. ^{13}C NMR spectrum of **1,3-Dibromo-4,6-bis(trifluoromethyl)benzene (1)**

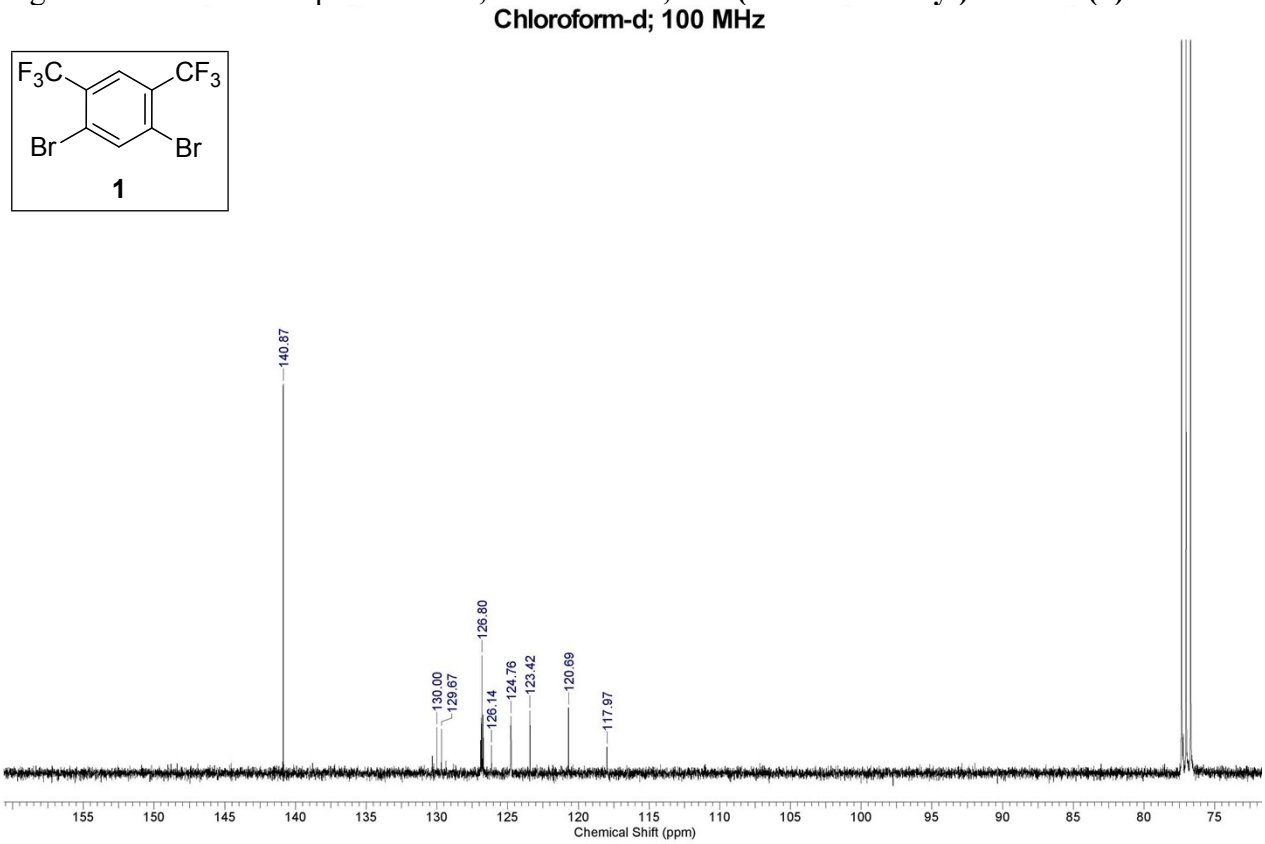

Figure S2-1. ^{1}H NMR spectrum of **4,6-bis(trifluoromethyl)resorcinol dibenzyl ether (2)**

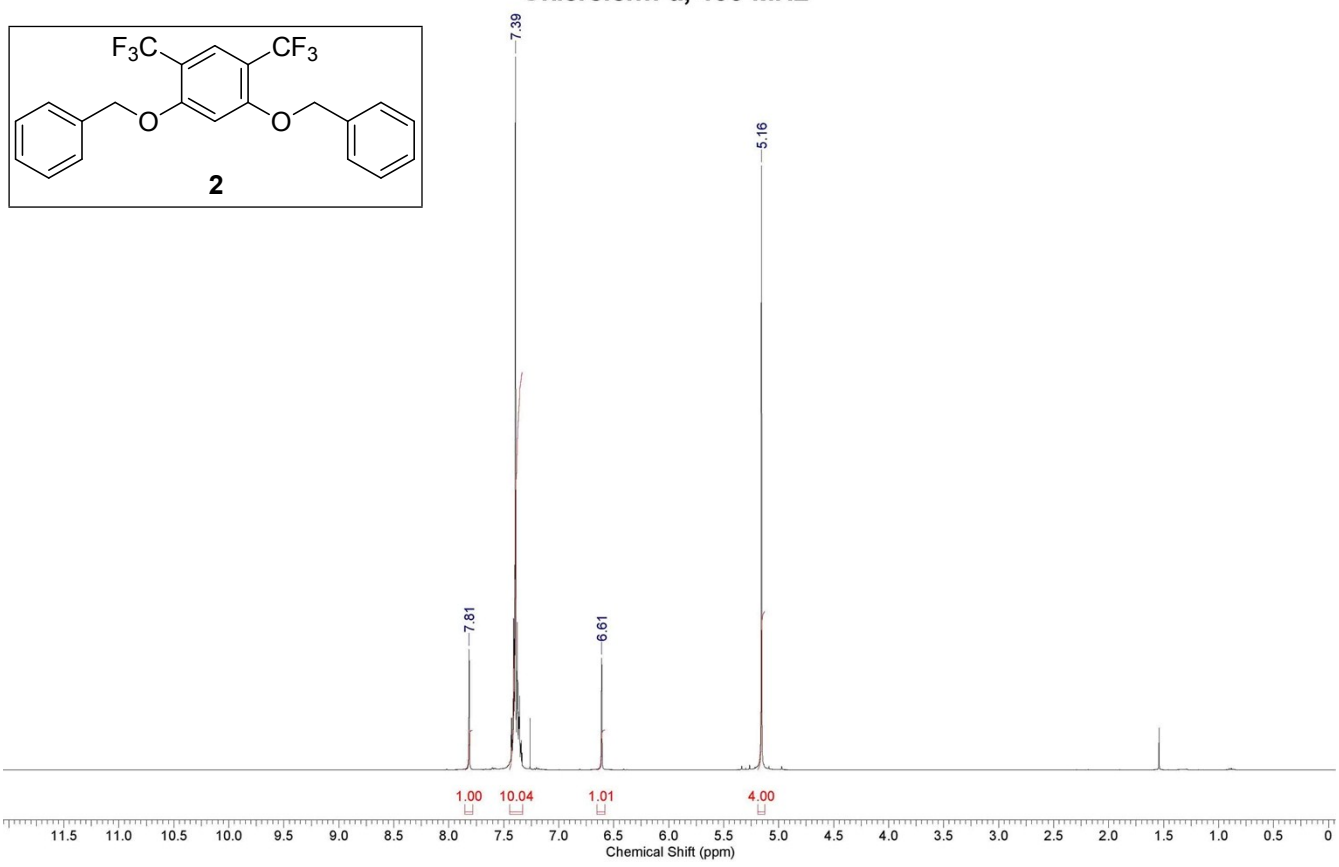

Figure S2-2. ^{19}F NMR spectrum of **4,6-bis(trifluoromethyl)resorcinol dibenzyl ether (2)**

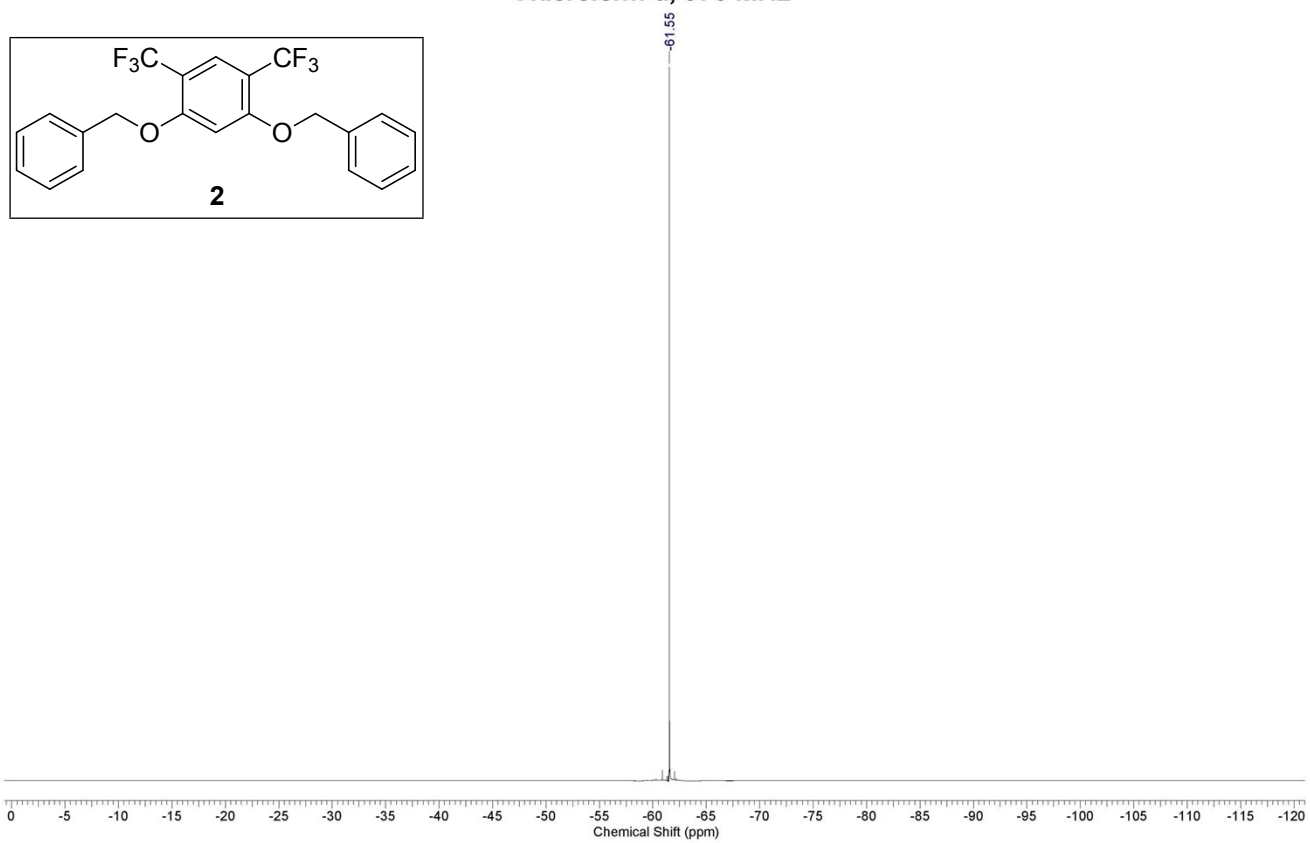

Figure S2-3. ^{13}C NMR spectrum of **4,6-bis(trifluoromethyl)resorcinol dibenzyl ether (2)**

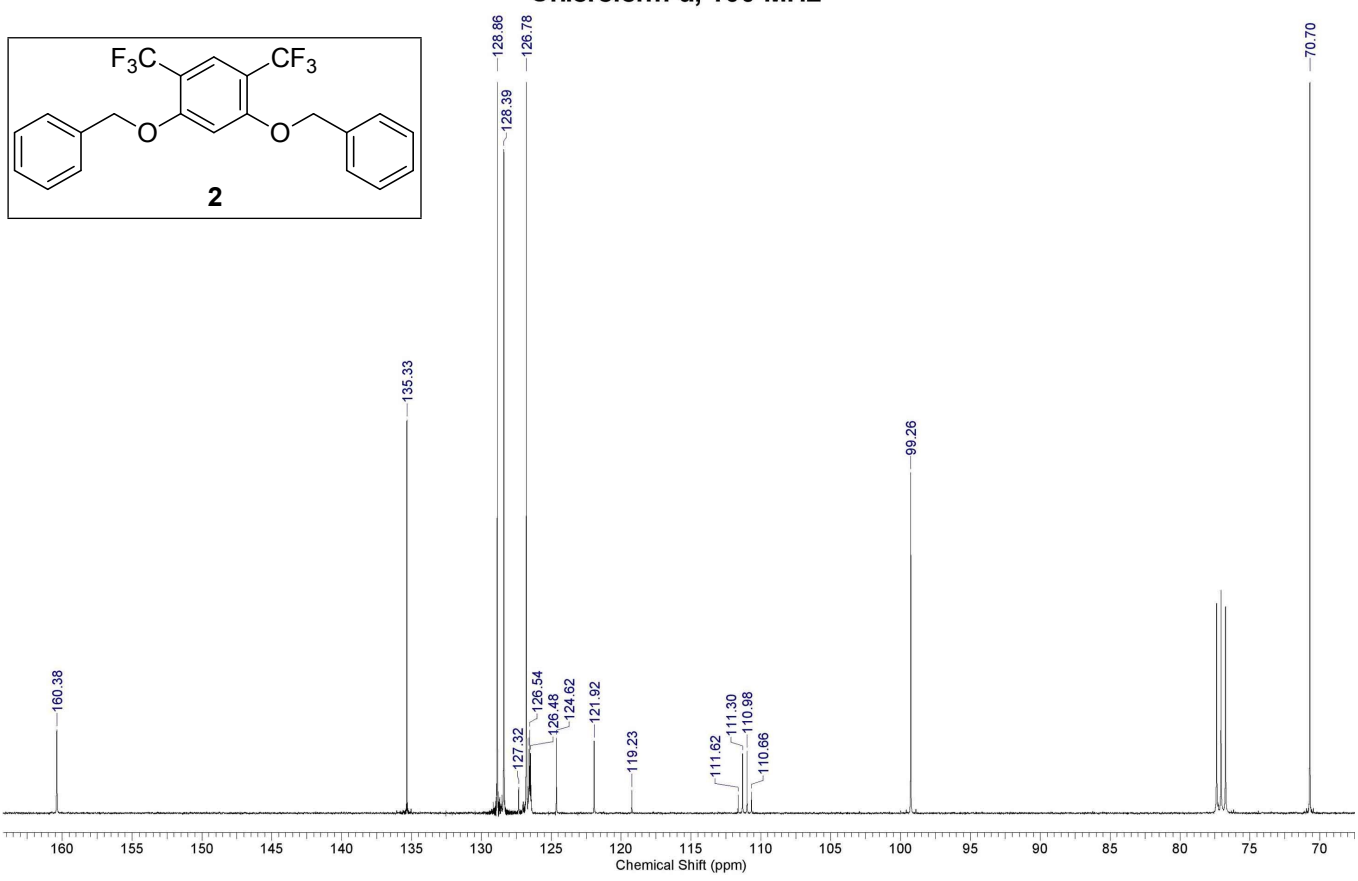

Figure S3-1. ^{1}H NMR spectrum of **4,6-bis(trifluoromethyl)resorcinol (3)**

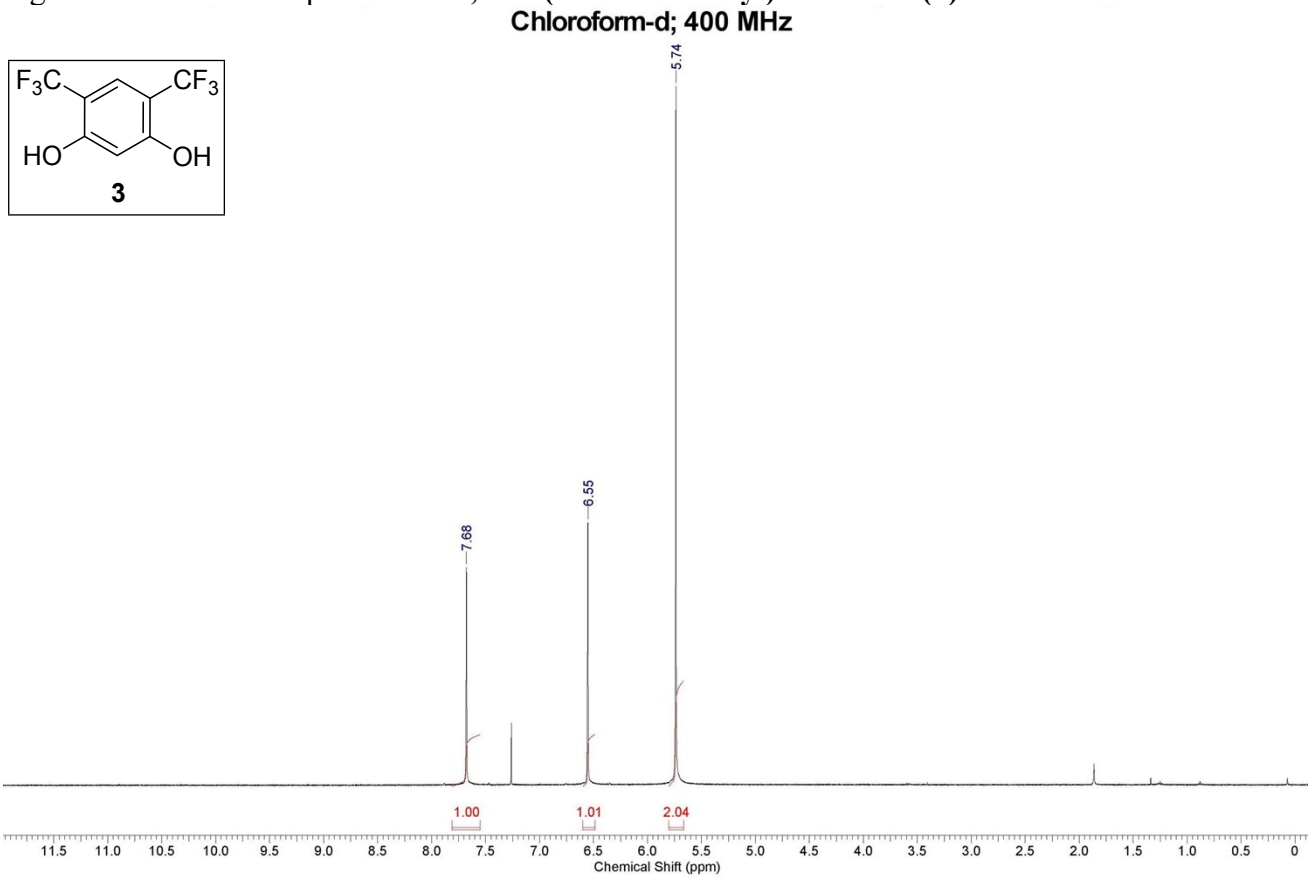

Figure S3-2. ^{19}F NMR spectrum of **4,6-bis(trifluoromethyl)resorcinol (3)**

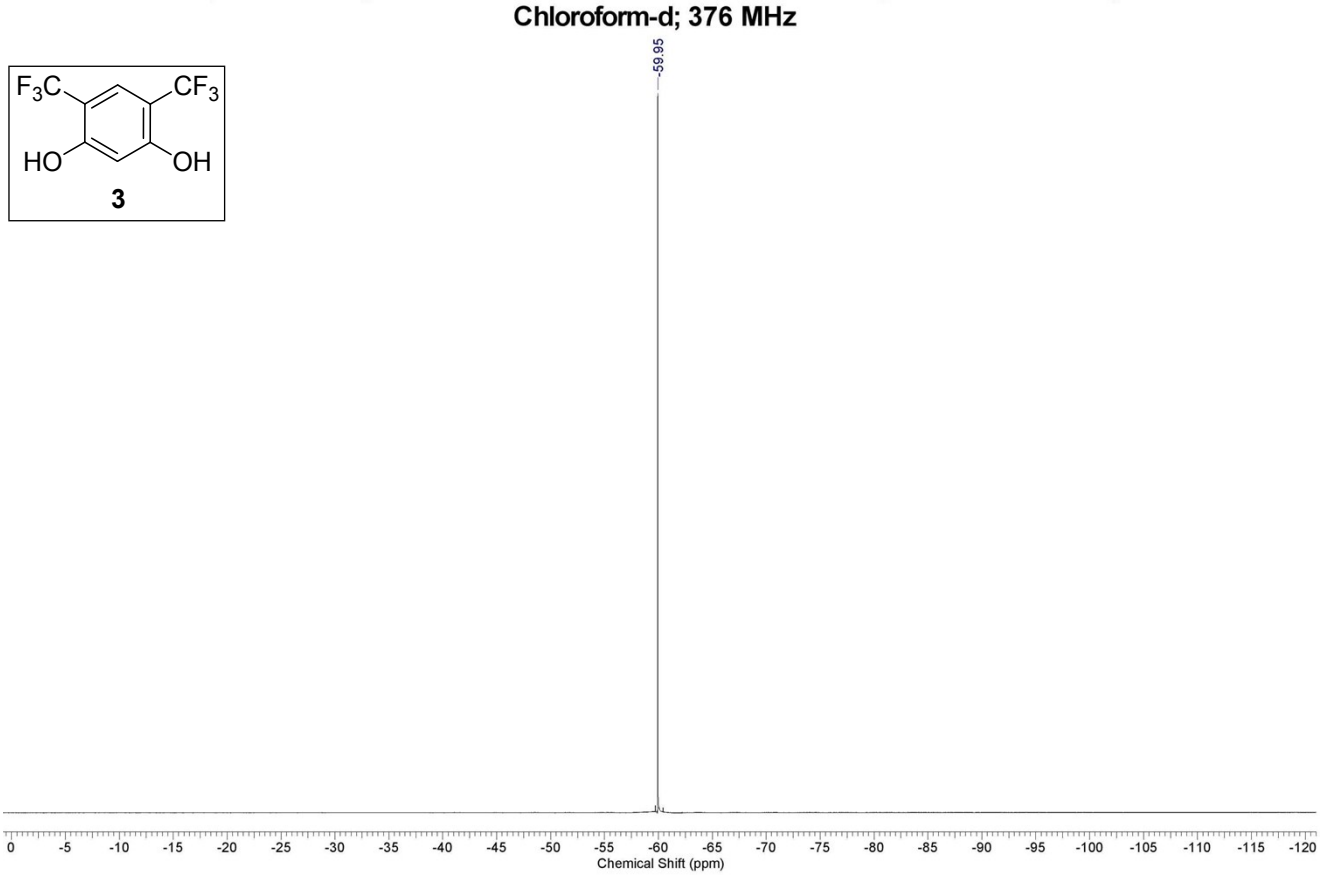

Figure S3-3. ^{13}C NMR spectrum of **4,6-bis(trifluoromethyl)resorcinol (3)**

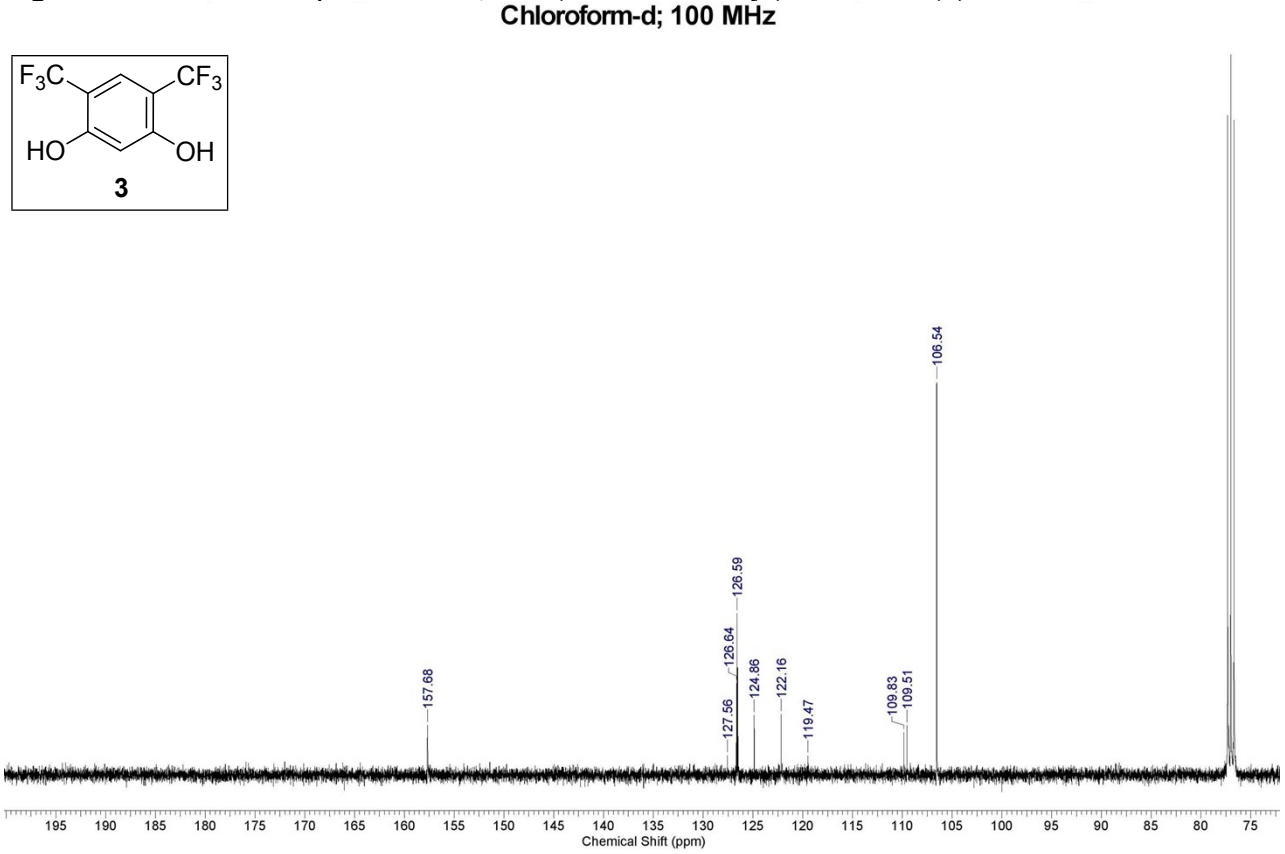

Figure S4-1. ^{1}H NMR spectrum of **((4,6-bis(trifluoromethyl)-1,3-phenylene)bis(oxy))bis(di-*tert*-butylphosphine) (4)**

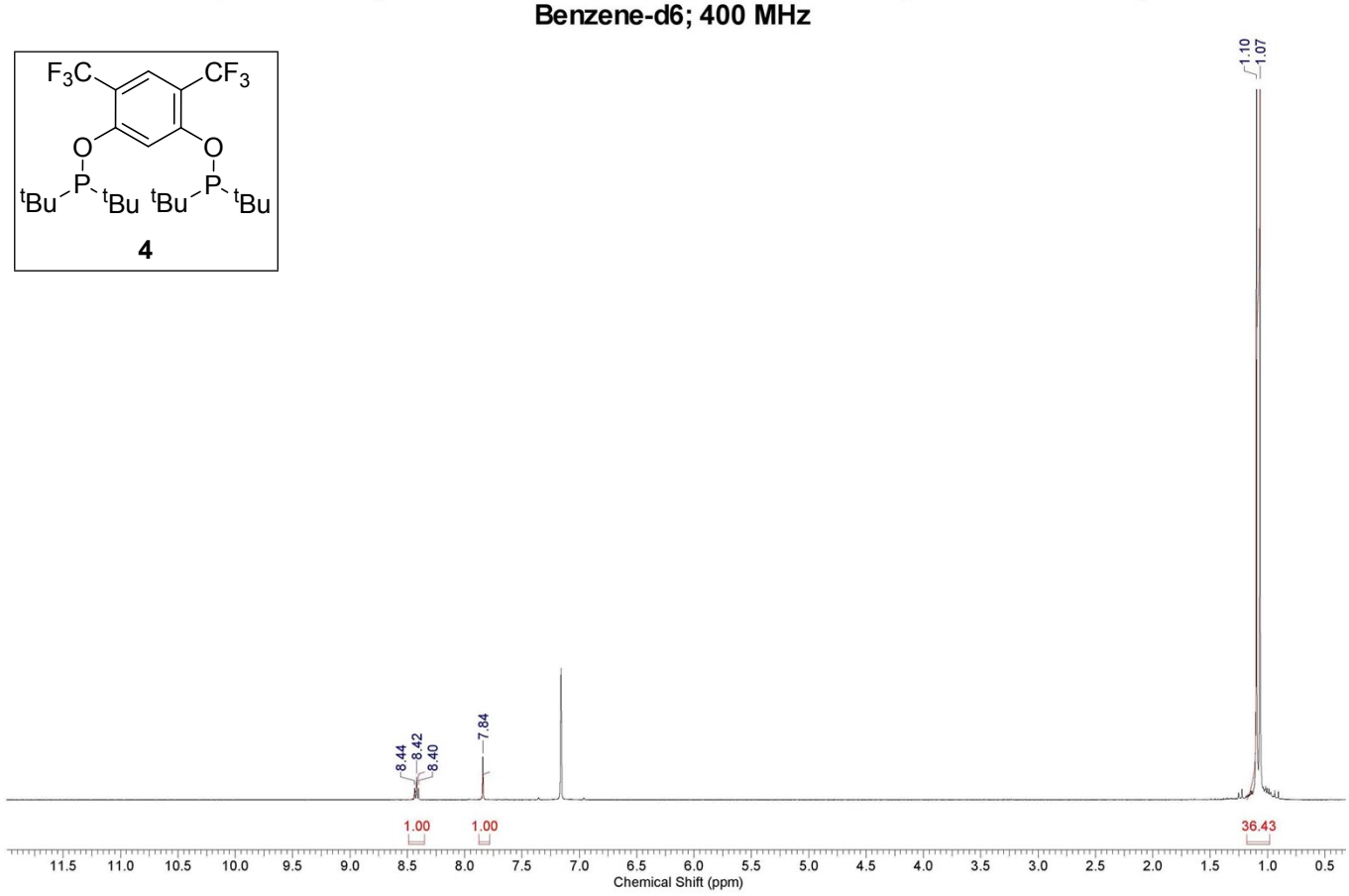

Figure S4-2. ^{19}F NMR spectrum of **((4,6-bis(trifluoromethyl)-1,3-phenylene)bis(oxy))bis(di-*tert*-butylphosphine) (4)**

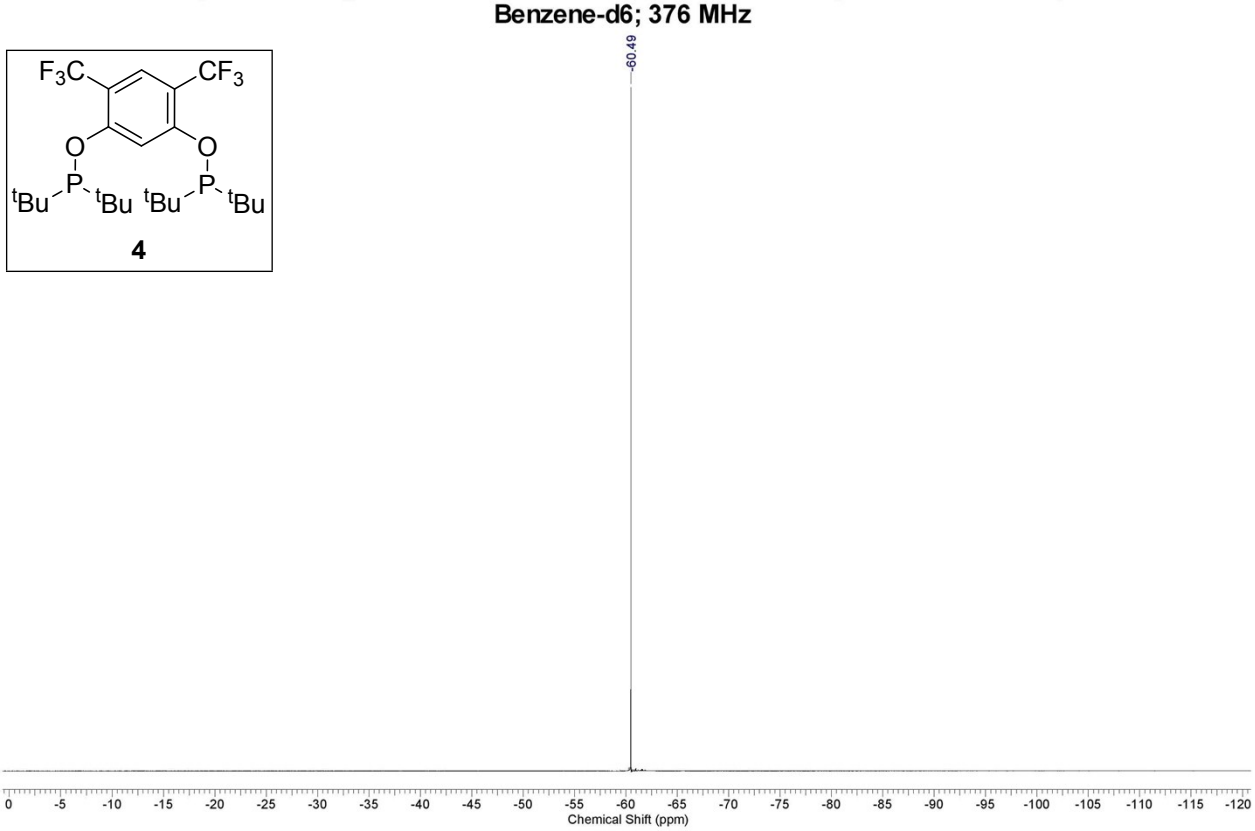

Figure S4-3. ^{31}P NMR spectrum of **((4,6-bis(trifluoromethyl)-1,3-phenylene)bis(oxy))bis(di-*tert*-butylphosphine) (4)**

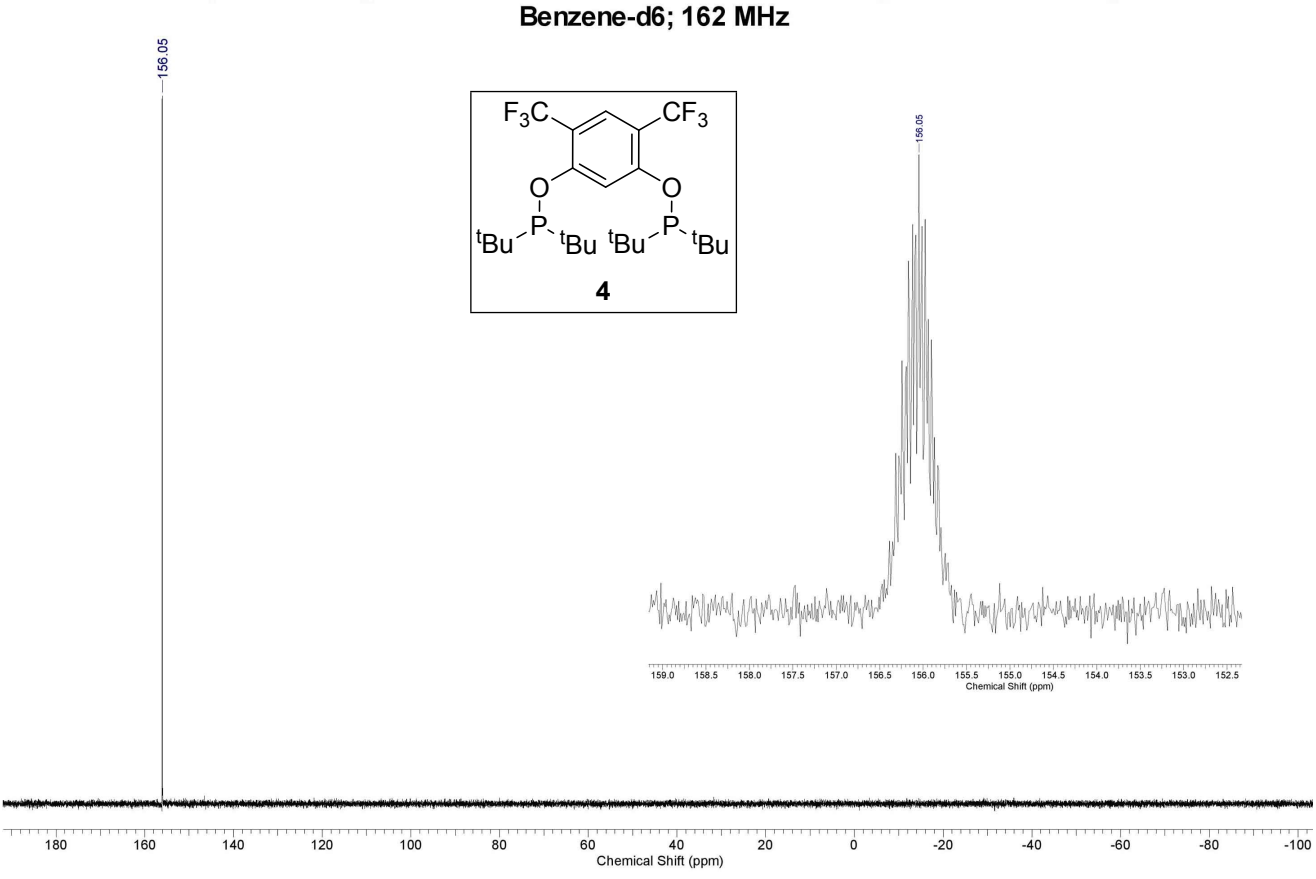

Figure S4-4. ^{13}C NMR spectrum of **((4,6-bis(trifluoromethyl)-1,3-phenylene)bis(oxy))bis(di-*tert*-butylphosphine) (4)**

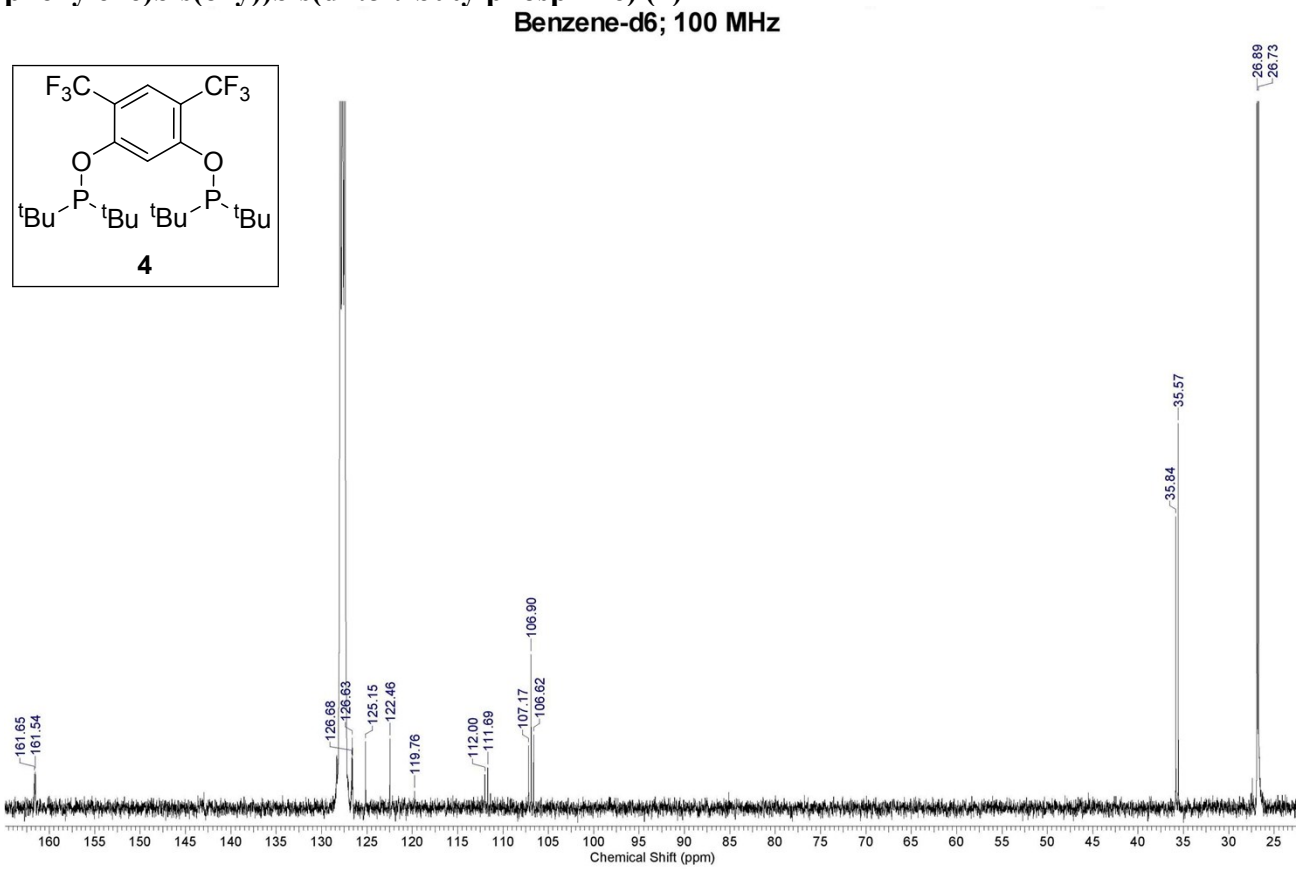

Figure S5-1. ^{1}H NMR spectrum of **CF_3(POCOP)IrHCl (5)**

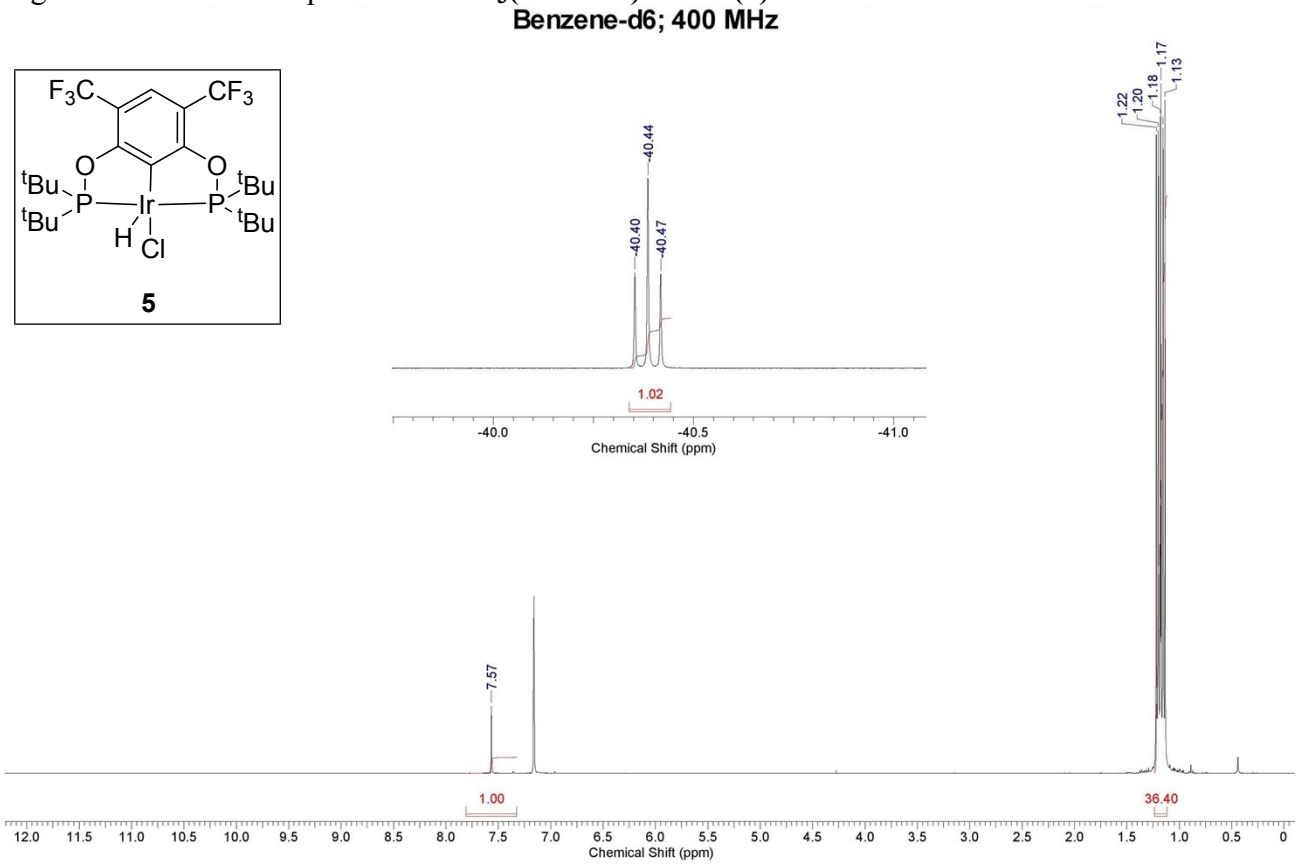

Figure S5-2. ^{19}F NMR spectrum of **CF_3(POCOP)IrHCl (5)**

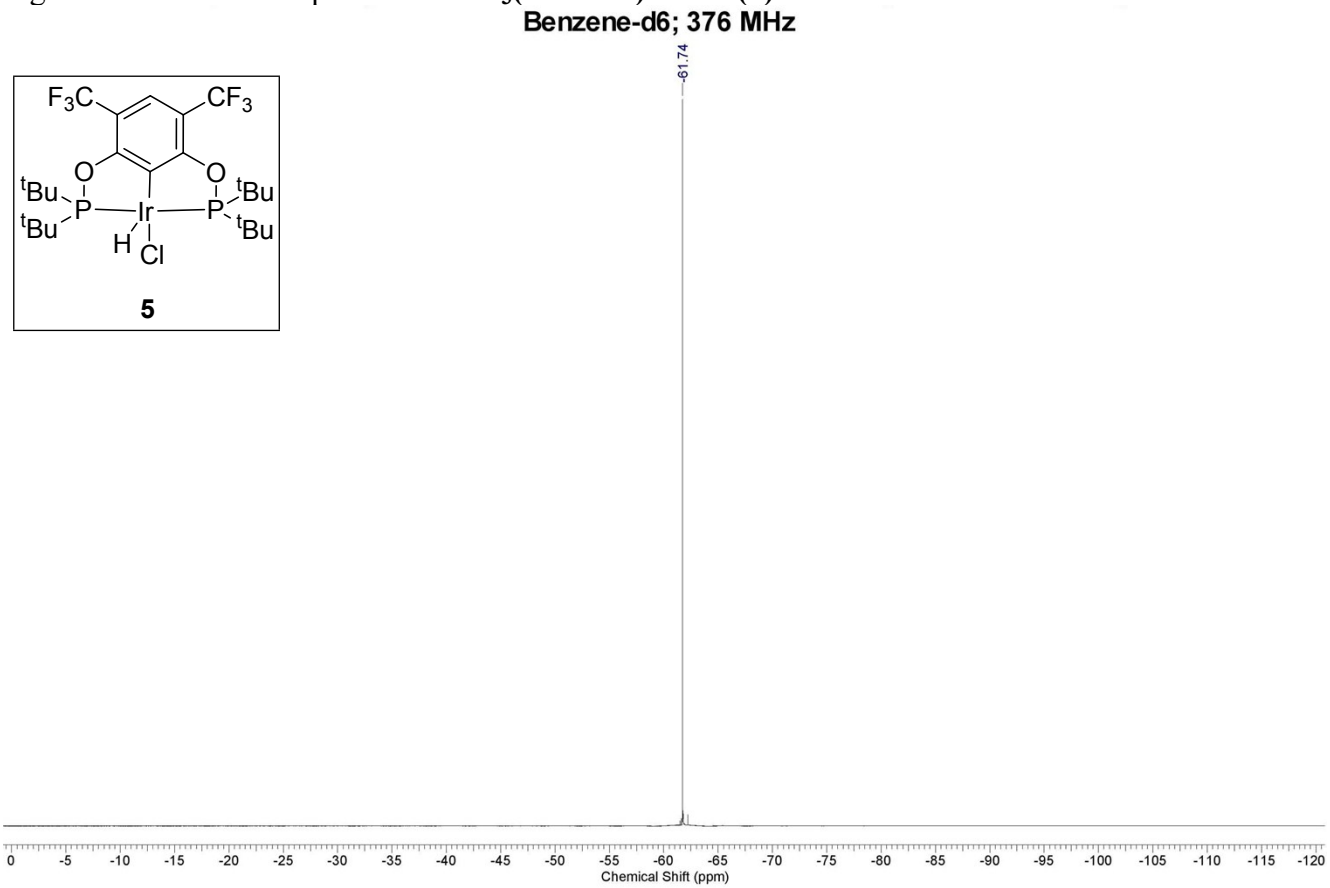

Figure S5-3. ^{31}P NMR spectrum of **CF_3(POCOP)IrHCl (5)**

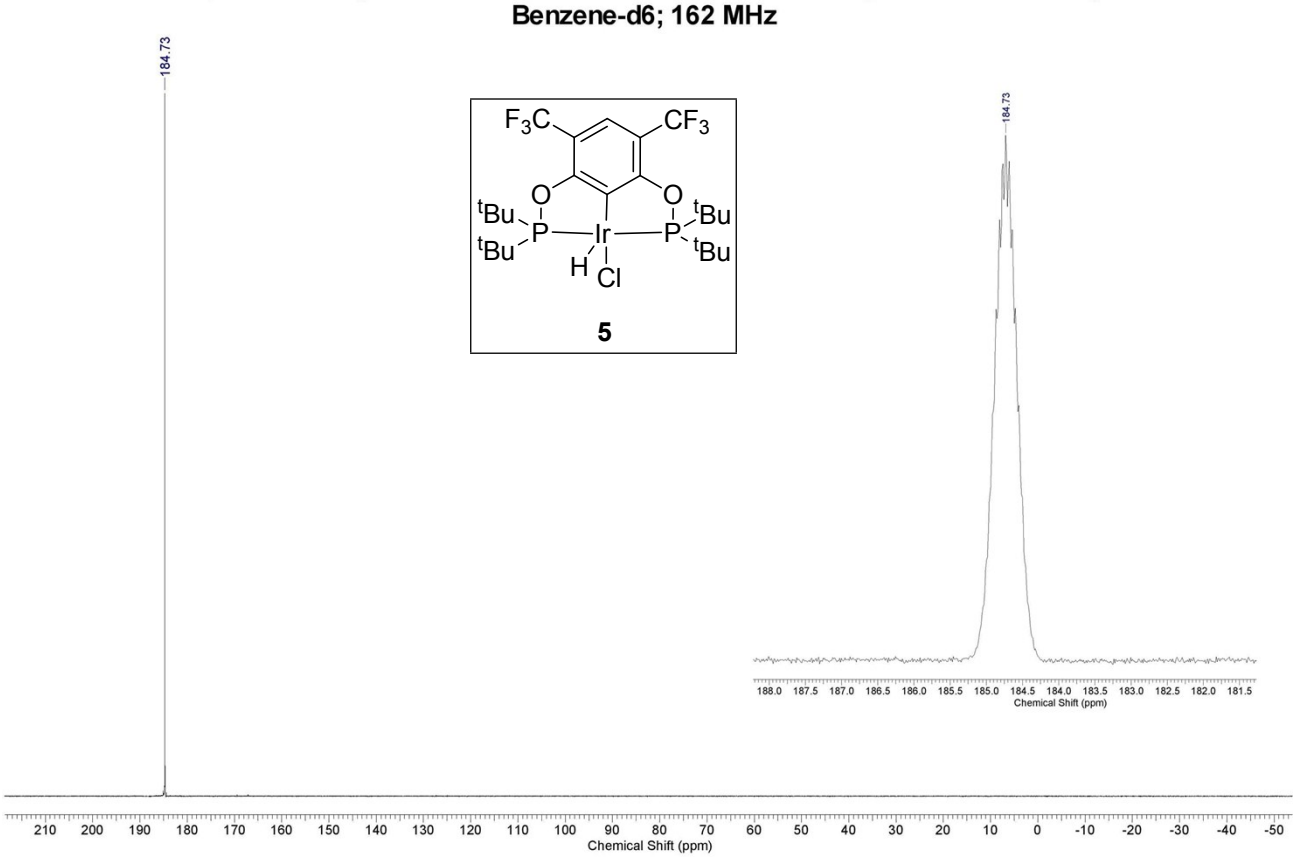

Figure S5-4. ^{13}C NMR spectrum of **CF_3(POCOP)IrHCl (5)**

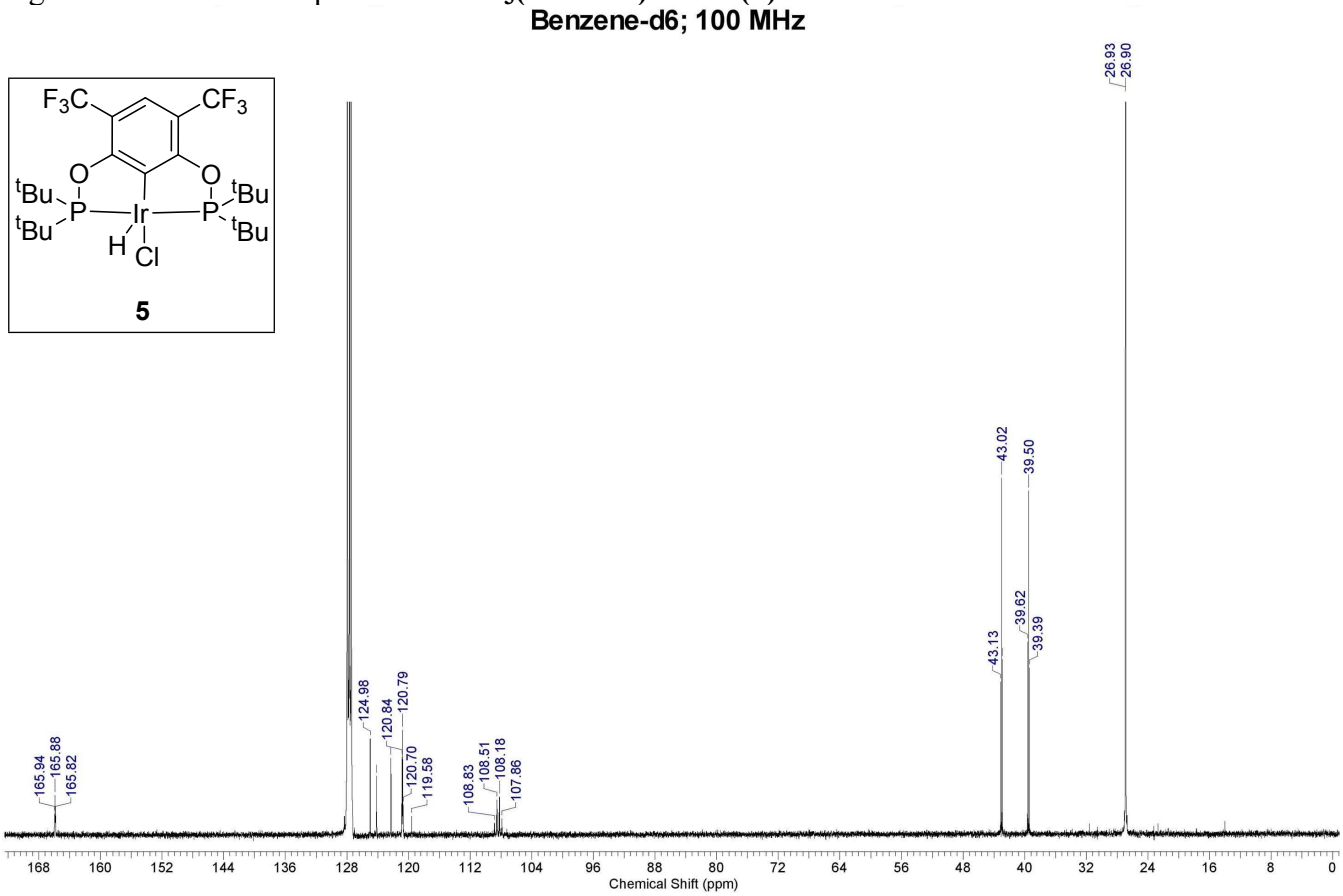

Figure S6-1. ^{1}H NMR spectrum of **CF_3(POCOP)Ir (7)**

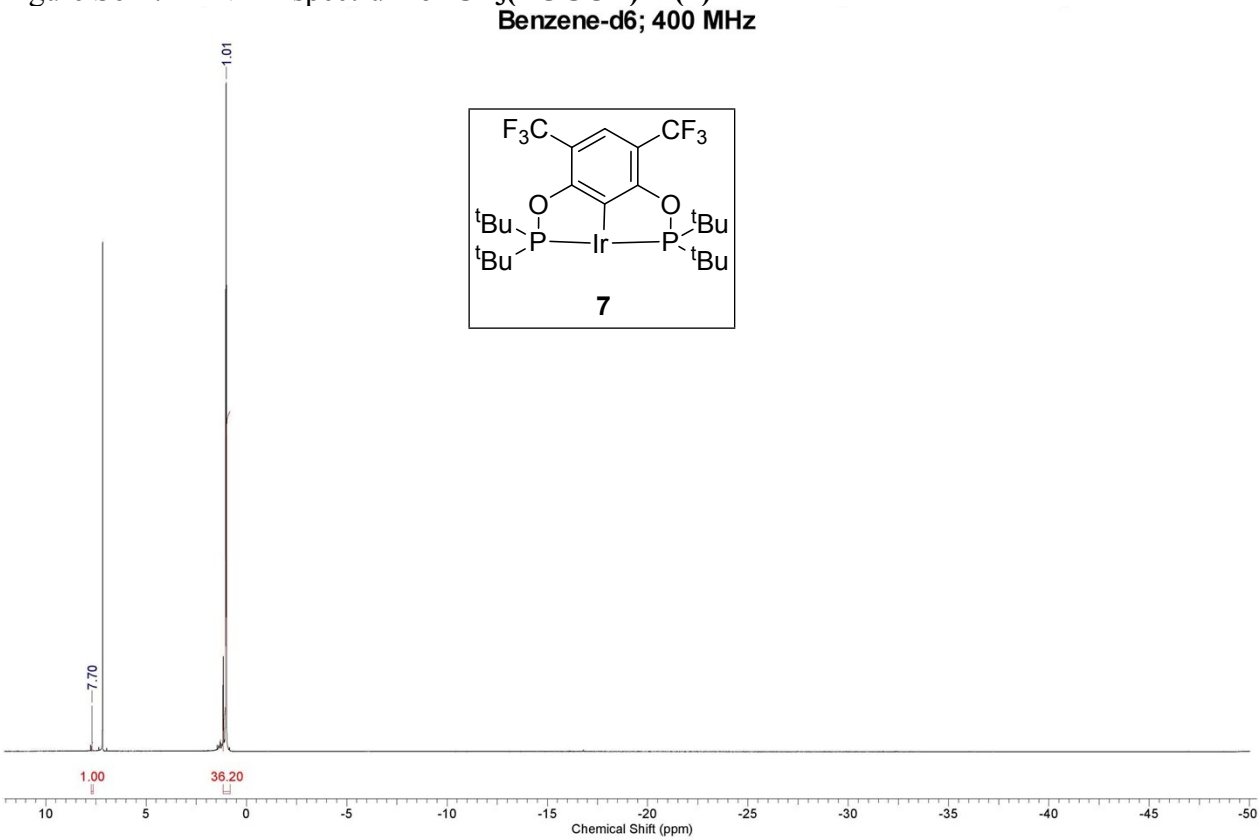

Figure S6-2. ^{19}F NMR spectrum of **CF_3(POCOP)Ir (7)**

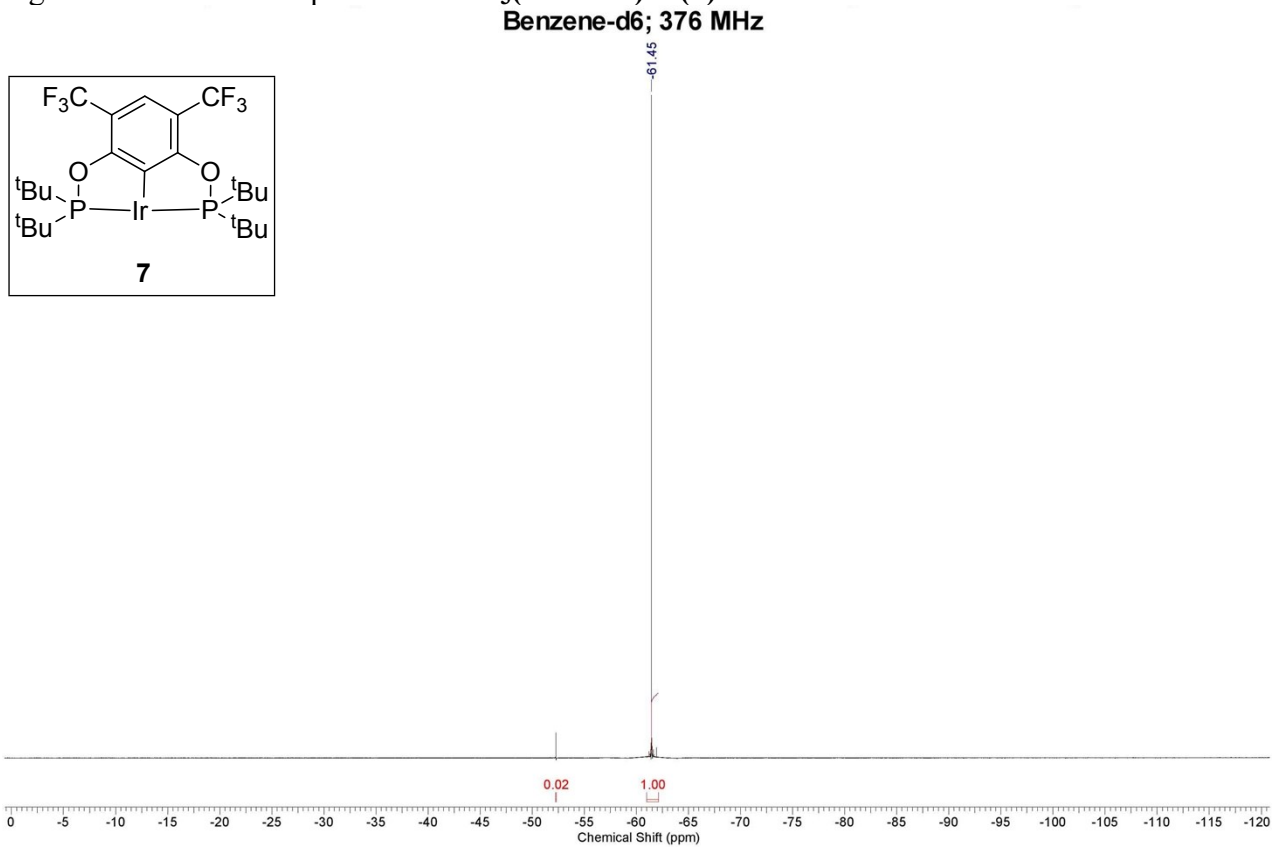

Figure S6-3. ^{31}P NMR spectrum of **CF_3(POCOP)Ir (7)**

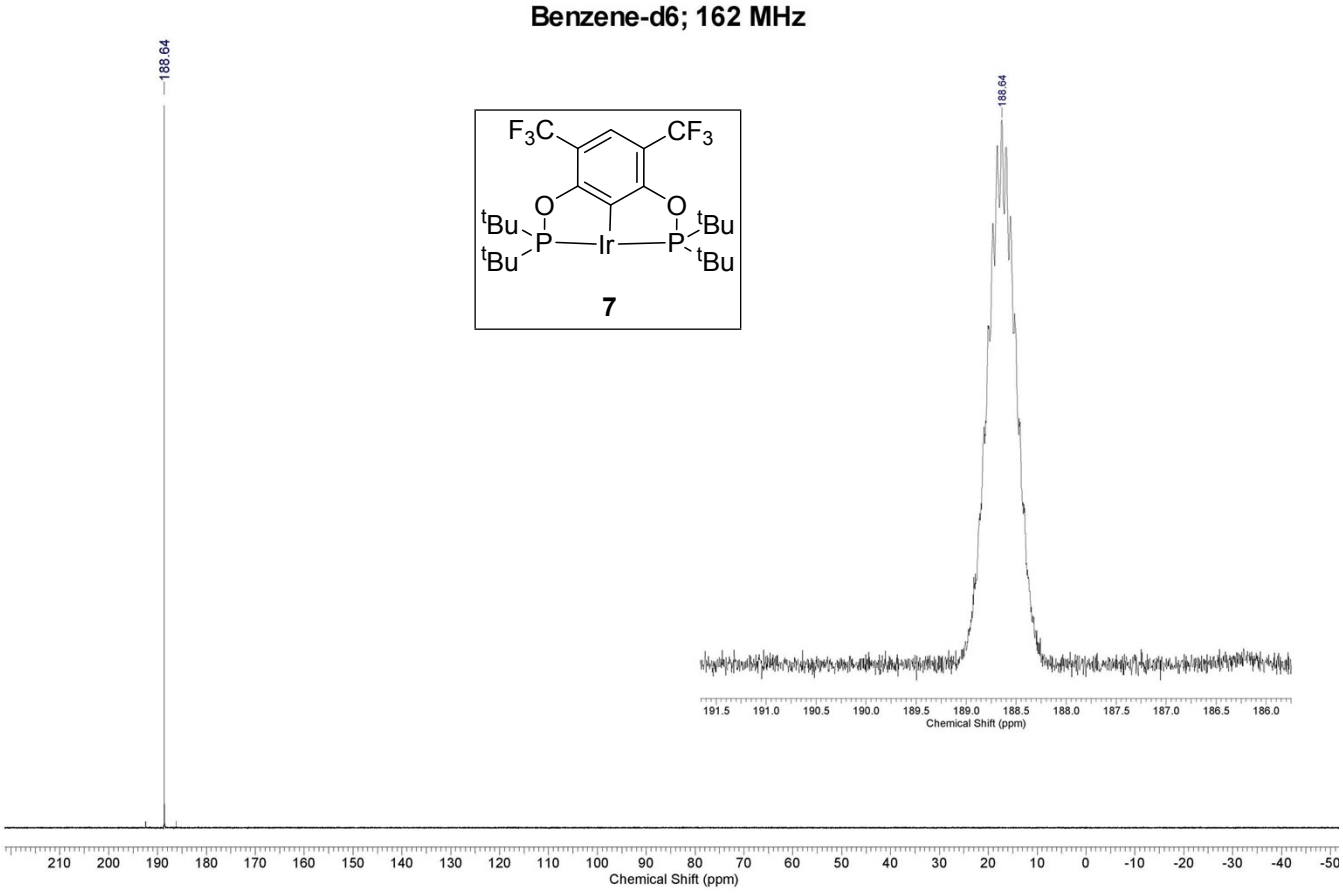

Figure S6-4. ^{13}C NMR spectrum of **CF_3(POCOP)Ir (7)**

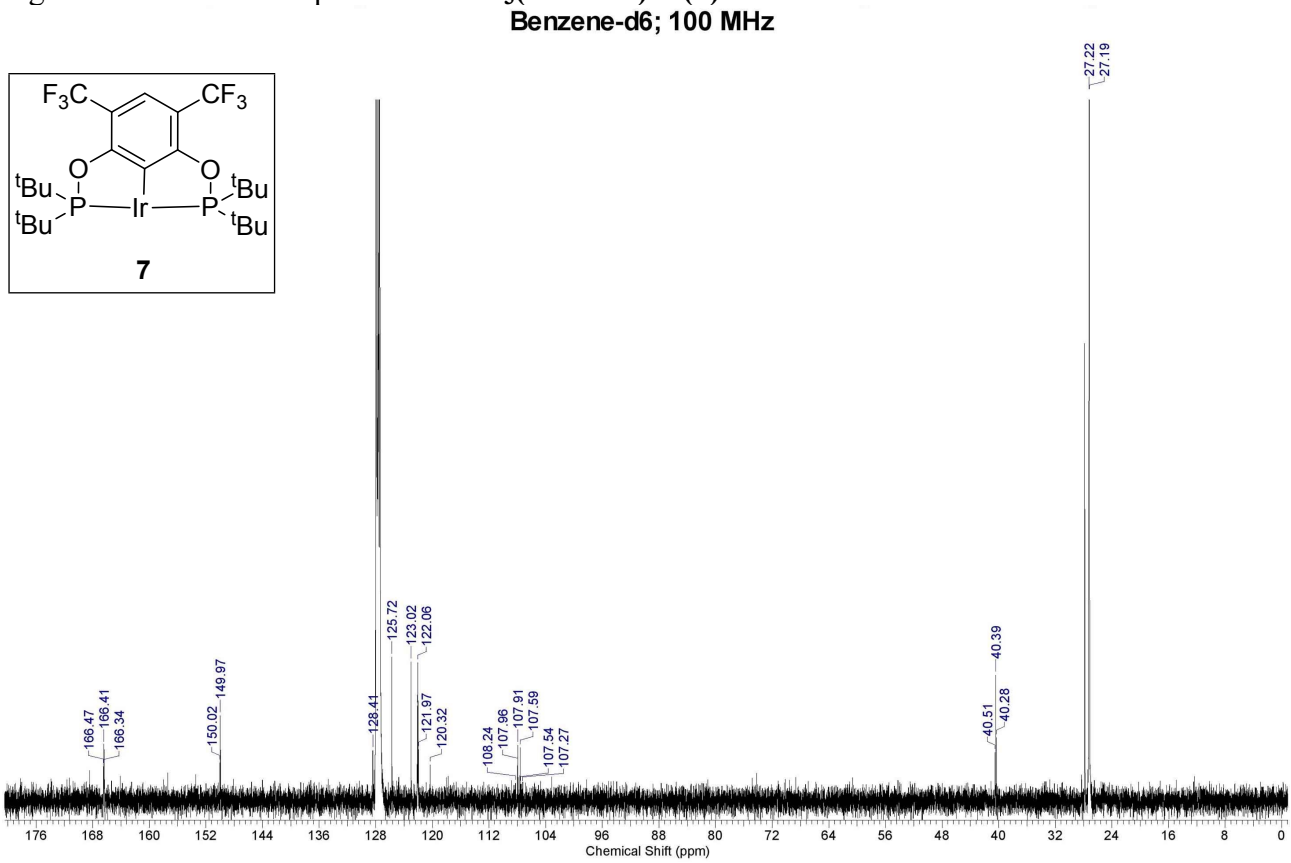

Figure S7-1. ^{1}H NMR spectrum of **CF_3(POCOP)IrCOE (8)** after drying in vacuo

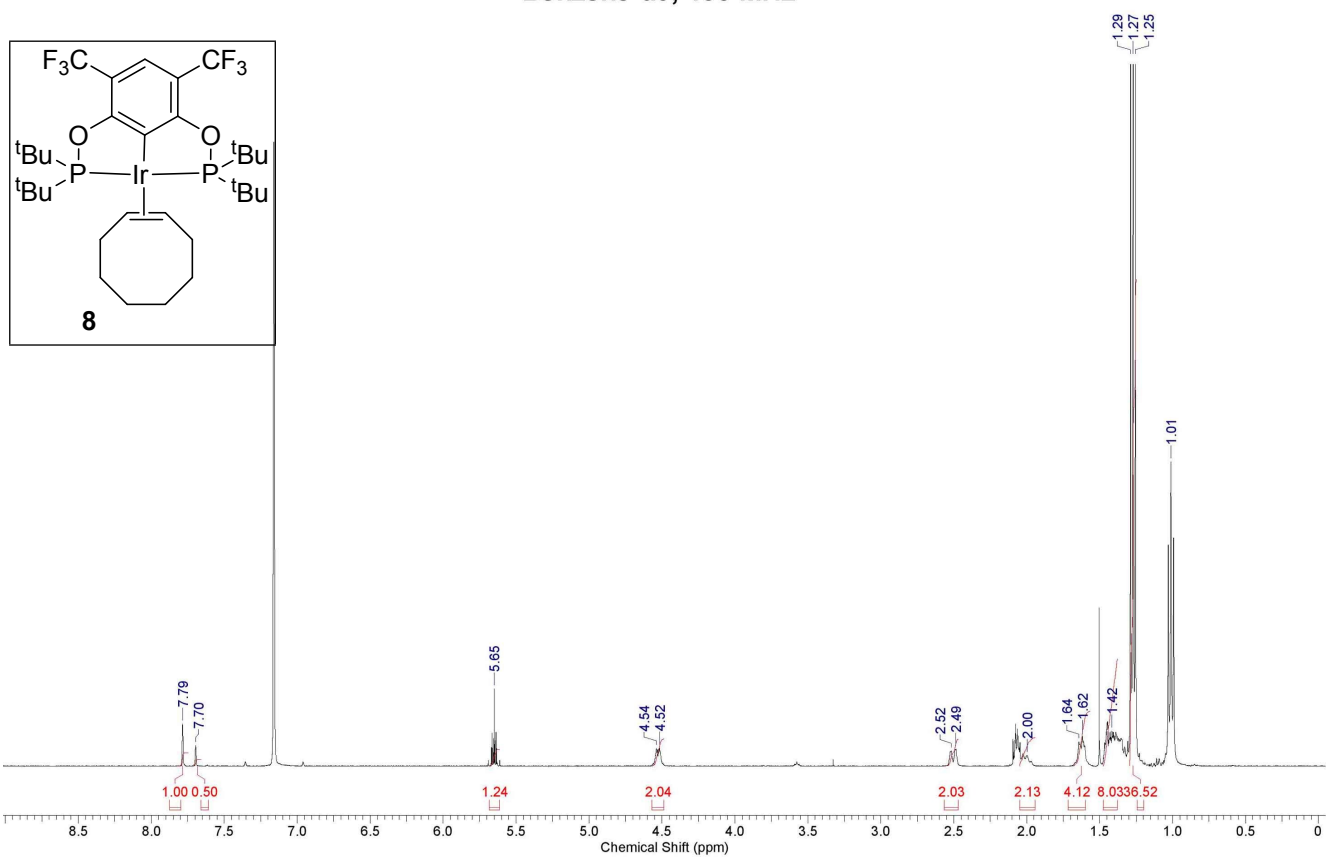

Figure S7-2. ^{19}F NMR spectrum of **CF_3(POCOP)IrCOE (8)** with 10-fold excess of COE

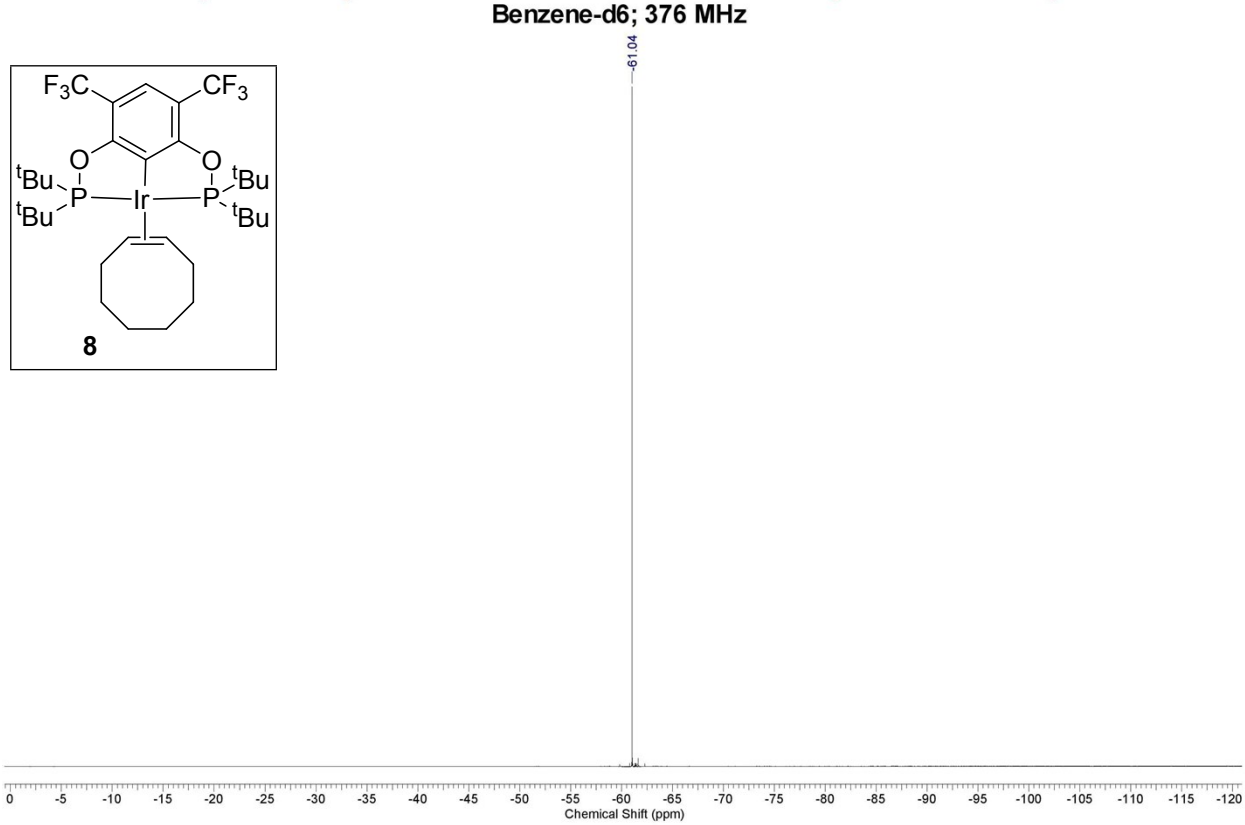

Figure S7-3. ^{19}F NMR spectrum of **CF_3(POCOP)IrCOE (8)** after drying in vacuo

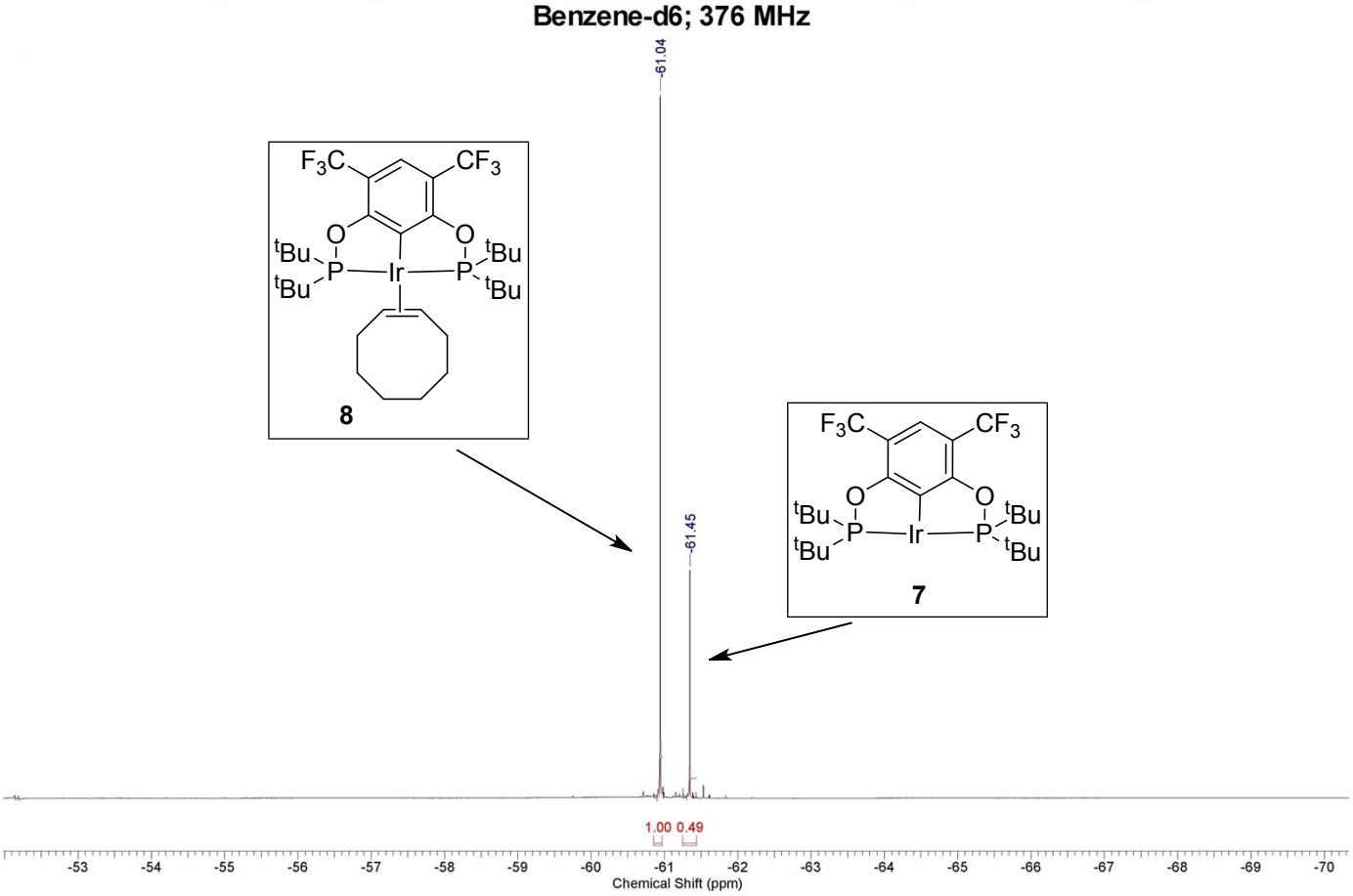

Figure S7-4. ^{31}P NMR spectrum of **CF_3(POCOP)IrCOE (8)** with 10-fold excess of COE

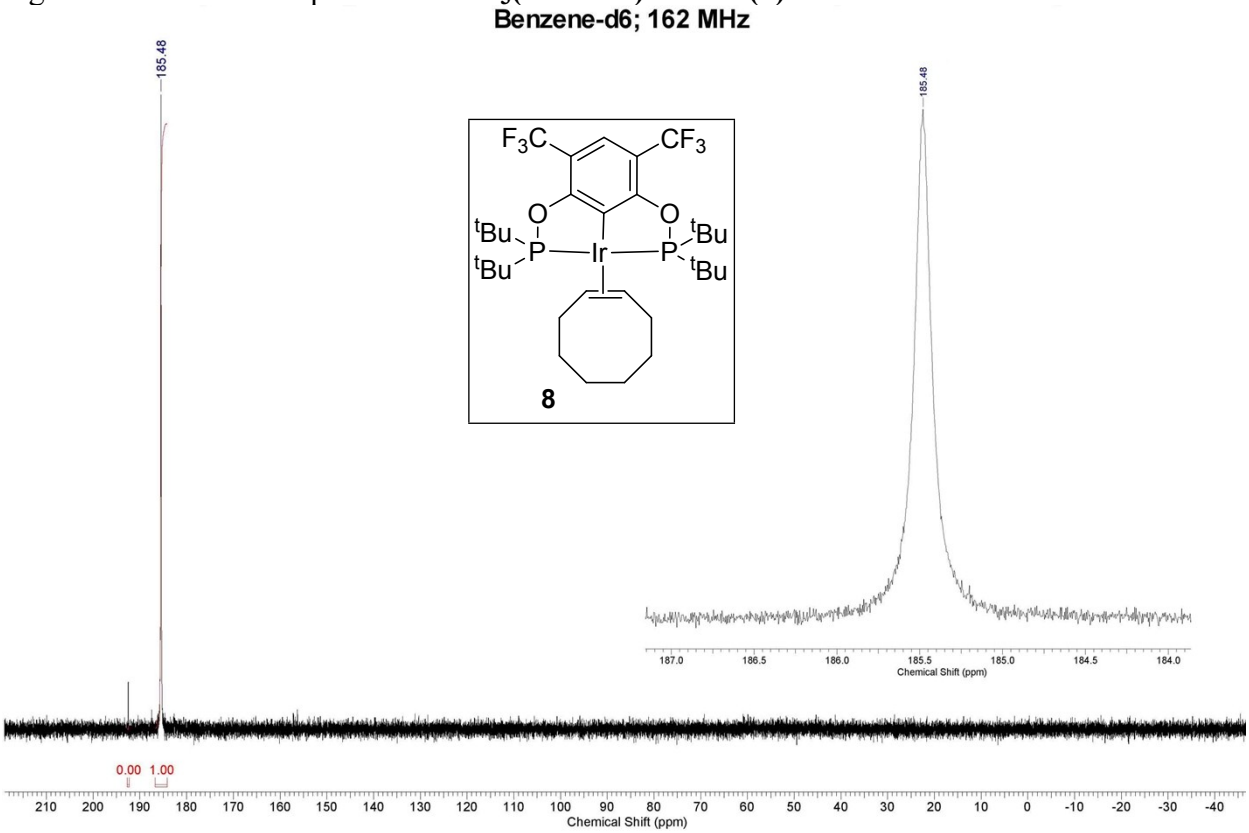

Figure S7-5. ^{31}P NMR spectrum of **CF_3(POCOP)IrCOE (8)** after drying in vacuo

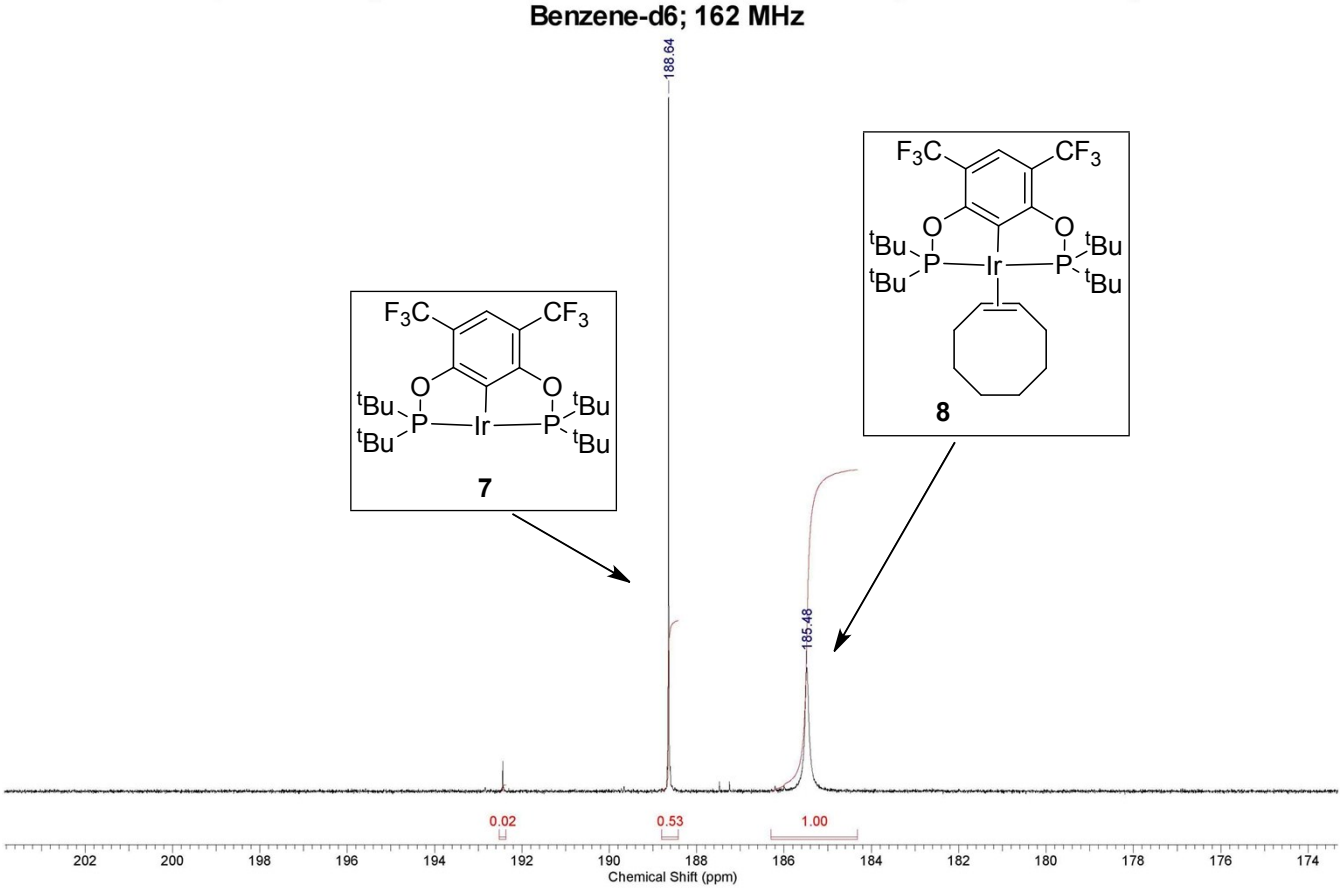

Figure S7-6. ^{13}C NMR spectrum of **CF_3(POCOP)IrCOE (8)** after drying in vacuo

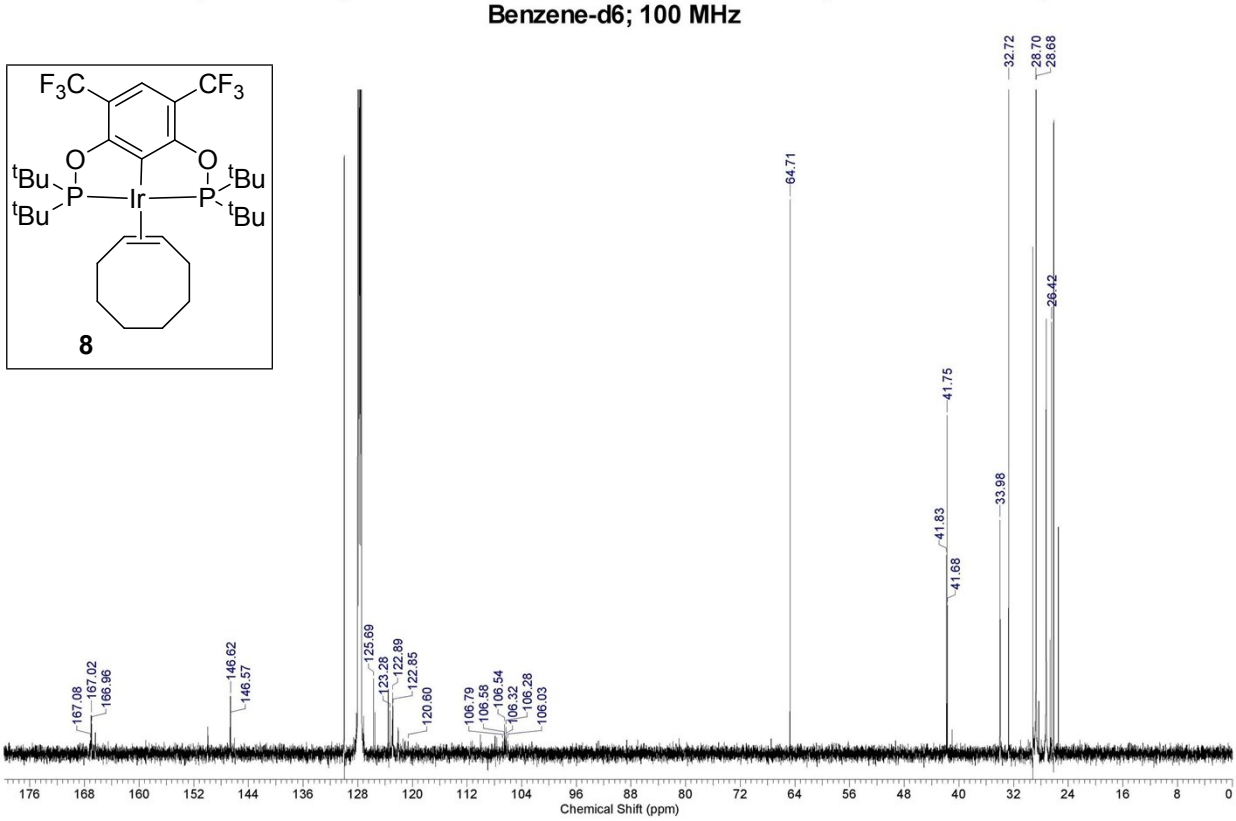

Figure S8-1. ^{19}F NMR spectrum of **CF_3(POCOP)IrTBE (9)** with 10-fold excess of TBE

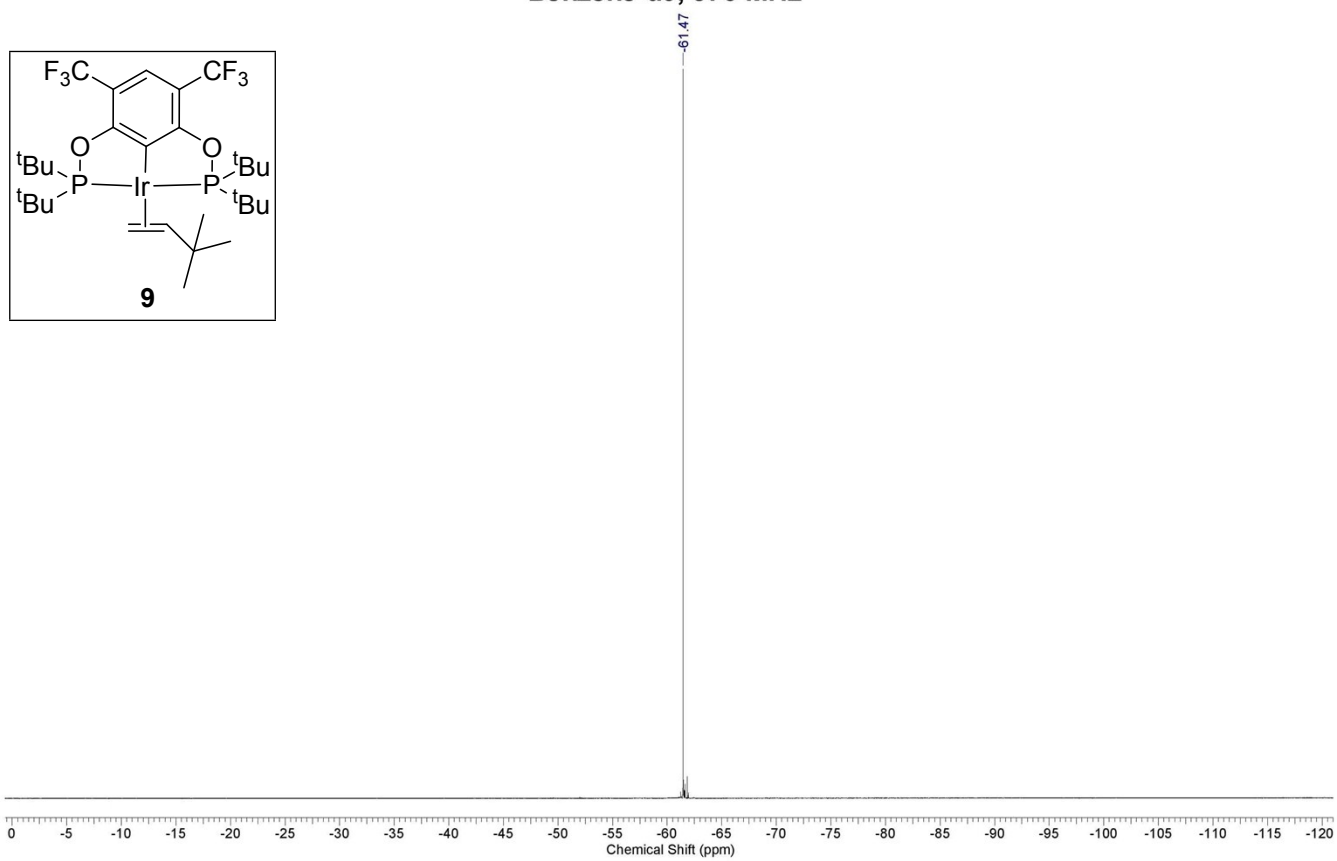

Figure S8-2. ^{31}P NMR spectrum of **CF_3(POCOP)IrTBE (9)** with 10-fold excess of TBE